CRYSTALLINE SILICON THIN-FILM SOLAR CELLS ON SILICON NITRIDE CERAMICS

S. Reber[1], G. Stollwerck[2], D. Osswald[3], T. Kieliba[1], C. Häßler[2]
[1]Fraunhofer Institute for Solar Energy Systems ISE, Oltmannsstr. 5, 79100 Freiburg, Germany
Phone: +49 (761) 4588-248, Fax: +49 (761) 4588-250, e-mail: reber@ise.fhg.de
[2]Bayer AG, Rheinuferstr. 7-9, R 52, D-47829 Krefeld, Germany
[3]Freiburger Materialforschungszentrum (FMF), Stefan-Meier-Str. 21, D-79104 Freiburg

ABSTRACT: Crystalline silicon thin-film (CSiTF) solar cells on foreign substrates can be a possibility to reduce cost for photovoltaics in the future. One important prerequisite for the so-called high-temperature approach is a substrate material which is able to meet both physical requirements and cost goals. Silicon nitride can meet these demands: it is stable at high temperatures up to 1700 K and can withstand thermal shocks up to 800 K.
This paper reports the preparation of CSiTF solar cells on specially developed Si_3N_4 ceramic substrates for the first time. Different types of Si_3N_4 ceramic wafers were coated with 10 µm of silicon by atmospheric pressure CVD (APCVD). This layer was recrystallized by a zone-melting step and epitaxially thickened to approx. 30 µm. Defect analysis of the layer surface and of cross sections was done in order to determine the crystallographic properties of the silicon layers, as well as mass spectroscopy to measure the concentration of transition metal impurities. A one-side contact solar cell process was applied to selected samples. The best cell achieved an efficiency of 9.4% with an excellent I_{sc} of 26.1 mA/cm^2 and a V_{oc} of 539 mV (best V_{oc}: 554 mV). Solar cell characterization was completed by measurements of dark current-voltage characteristics, spectrally resolved light beam induced current mapping, and external quantum efficiency measurement.
Keywords: Silicon Nitride - 1: c-Si - 2: Thin-Film - 3

1 INTRODUCTION

The high-temperature approach for preparation of crystalline silicon thin-film (CSiTF) solar cells has the potential to reach efficiencies higher than 19% [1]. Even when using zone-melting recrystallization (ZMR), efficiencies exceeding 16% have been achieved [2]. However, if no lift-off techniques shall be applied, there are some stringent requirements on the substrate. First of all, the cost for the substrate has to be compatible to the cost goals for the CSiTF solar cell. Literature indicates a maximum substrate cost of 25-50 €/m^2 [3]. Of course, also physical requirements have to be met: the substrate has to be resistant against high temperatures and its thermal expansion coefficient (TEC) must fit well to that of silicon for example. Furthermore, if zone-melting recrystallization is used, it possibly has to bear large temperature gradients. Ceramics and silicon are able to withstand the required temperatures above 1000 °C without deforming or significant outgasing of impurities. Up to now, research was done on graphite [4], SiSiC [5], SiAlON [6], Al_2O_3 [7], mullite [8] and low cost silicon [9].

In this work, silicon nitride ceramics was investigated for CSiTF solar cell purposes: it is stable at high temperatures with a decomposition temperature of 2170 K, it can withstand thermal shocks up to 800 K and keeps its high mechanical stability up to 1700 K. The TEC of Si_3N_4 is 3.2 - 3.8·10^{-6} K^{-1} and thus only slightly smaller than that of silicon (3.9·10^{-6} K^{-1}). The chemical inertness of Si_3N_4 is excellent and impurities are tightly bound in the ceramics structure. The open porosity usually is below 3 % with pore diameters smaller than 1 µm. This allows deposition of thin, compact intermediate layers as diffusion barriers. Two main production routes are possible for Si_3N_4: reaction binding and powder sintering. More details about Si_3N_4 can be found in [10] and [11] for example.

2 EXPERIMENT

The first series of Si_3N_4 wafers had a size of approx. 50 mm (circular or square) and were made either by sintering or by reaction binding. The preparation was done on a laboratory scale by the CFI Ceramics for Industry GmbH & Co.KG, Rödental, Germany. All samples received a final surface treatment to achieve a mirror-like surface. Three different types of Si_3N_4 wafers were prepared: a non-conductive species with a 2.1 µm thick plasma-enhanced CVD (PECVD) SiO_2–SiN_x–SiO_2 intermediate layer (sample type A), a non-conductive species with an in-situ grown, 20 µm thick 'thermal' silicon dioxide layer (sample type B) and a conductive species without intermediate layer (sample type C).

Homogeneous, fine-grained Si layers of approx. 10 µm thickness and a doping level of 5·10^{18} at/cm^3 could be grown without any whiskers by an APCVD silicon deposition. All samples then were coated with a 2 µm thick PECVD SiO_2 layer to prevent balling–up during ZMR performed subsequently.

The results of the ZMR did strongly depend on the sample type: only the samples of type A showed a defined melting and solidification front, resulting in the structure typical for ZMR with grains of several millimeters in width and several centimeters in length (see Fig. 1). For all other sample types, either balling-up or columnar recrystallization without formation of large grains occurred.

After wet chemical removal of the capping layer by hydrofluoric acid and a slight surface etch of the silicon layer using CP133 , the active solar cell silicon layer was deposited epitaxially, again by APCVD. Its thickness was chosen to approx. 30 µm with a doping level of 2·10^{16} at/cm^3.

The samples were characterized with respect to defect structure, composition and electrical properties. Solar cells were prepared from samples of type A, B and C

using a standard one-side contact cell process as described in [12]. Some of the samples were surface-textured prior to solar cell processing by anisotropic wet chemical etching resulting in a random pyramid surface structure.

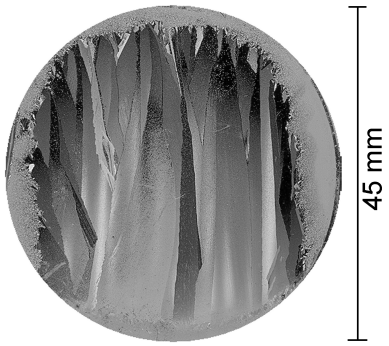

Fig. 1: Photograph of a silicon layer on Si_3N_4 ceramics of type A after ZMR and silicon epitaxy.

3 RESULTS

3.1 Defect analysis

After the solar cell process, a defect analysis was carried out. The interface of ceramics and silicon layer as well as the crystal structure of seeding and epitaxial silicon layer was examined using cell surfaces and cross sections of each sample type.

a) Non-conductive Si_3N_4 substrates with PECVD intermediate layer (type A)

This sample type led to the best solar cells. The epitaxial silicon layer has a scaly but well ordered surface. Most remarkable were microscopic cracks on some samples, which were spread out over the whole area, with a width of 2–3 µm. The corresponding part of the cross section (see Fig. 2) gave evidence that these cracks penetrate the whole silicon layer structure down to the intermediate layer. Their origin probably is the slight discrepancy of the TEC of silicon and silicon nitride, which presumably leads to different shrinking during the cool-down period, resulting in a gap-like crack geometry. There are strong indications which support that this happened after silicon epitaxy. Although the emitter fingers of the sample investigated partly crossed crack lines, it did show photovoltaic activity, so the cracks must have been present before emitter diffusion.

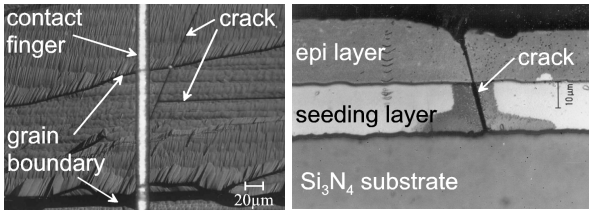

Fig. 2: Nomarski micrographs (left: surface, right: cross section) of a sample of type A.

b) Non-conductive Si_3N_4 substratse with thermal SiO_2 intermediate layer (type B)

The interface of non-conductive ceramics with thermal intermediate layer and silicon layer is completely different from the interface of the samples described previously. Large voids and indents in the 20 µm thick SiO_2 layer were filled with silicon either during seeding layer deposition or during ZMR. The irregularity of this interface may be the reason for the unsatisfying recrystallization step.

The overall crystal quality of this kind of sample is rather poor: compared to the samples with PECVD intermediate layer, even more cracks in the form of a network are present. In addition, they were unintentionally filled or overgrown with silver during the electroplating. They probably cause severe shunts, but at least supplementary shadowing losses. The top view of the surface reflects the bad crystal quality with a high number of growth defects and with small grains only.

c) Conductive Si_3N_4 substrates (type C)

No cracks could be observed in the silicon layers of this sample type, so the TEC seems to fit better to that of silicon. The large amount of non-Si_3N_4 material which fills up the pores of this ceramics type could be the reason for this behavior. Contrary to the samples of type A, the epitaxial silicon layer of type C is characterized by a higher overall defect density, as cross sections and surfaces show. Dislocations and small grains are distributed homogeneously over the sample area, thus providing a high density of recombination centers in the active solar cell layer.

3.2 Mass spectroscopy analysis

The chemical composition of the silicon layers on top of the various substrate types was examined by glow discharge mass spectroscopy.

Since all samples had a p^+p-structure, the interface between epitaxial layer and seeding layer is characterized by a significant increase of the boron signal within a few test values. The following conclusions can be made from the measured concentration profiles:

In samples of type A, the elements iron, chromium and titanium could be detected with concentrations in the range of 0.1–1ppma. This value decreases in the seeding layer and is below the detection limit at the interface of seeding layer and epitaxial layer. Therefore, the epitaxial layer is free of impurity metals within the measurement accuracy.

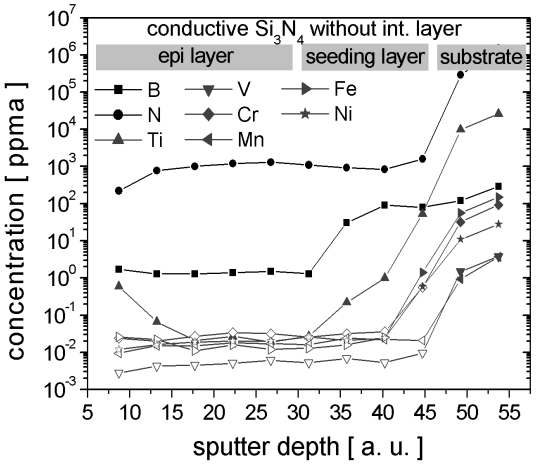

Fig. 3: Concentration profile of a type C sample measured by glow discharge mass spectroscopy. Non-filled symbols represent the detection limit.

In samples of type B also the transition metals iron, chromium, titanium and nickel are present. Concentrations are in the range of 0.1–1 ppma in the seeding layer and decrease beneath the detection limit towards the epitaxial layer. In contrast to the other sample types, a distinct high oxygen concentration can be found in the seeding layer, maybe caused by enhanced solution of oxygen from the porous thermal SiO_2 layer during ZMR.

In contrast to samples of type A and B, a significantly higher concentration of transition metal impurities can be detected inside the conductive Si_3N_4 substrate of the samples of type C (see Fig. 3): concentrations of vanadium, manganese, chromium and iron is two orders of magnitude higher, titanium even five. However, the concentration of all transition metals is below the detection limit in both seeding and epitaxial silicon layer, with the exception of titanium. Although its concentration decreases strongly with increasing seeding layer thickness, there are significant test values all across the silicon layer, about 0.1-1 ppma in the seeding layer and 0.02 ppma in the epitaxial layer. Most remarkable is a slight increase of the titanium concentration towards the upper surface of the epitaxial layer up to 0.6 ppma, which might be an indication for segregation to the surface during the process of base epitaxy. The amount of this contamination should impede any photovoltaic activity due to effective recombination at the titanium traps in the band gap.

3.3 Solar cell results and electrical properties

The characteristic parameters of dark and illuminated solar cells were measured after both remote plasma hydrogen passivation and antireflection coating. The best cell was calibrated in the Fraunhofer ISE calibration laboratory.

The high fill factors of the monocrystalline reference samples prove, that no contamination of the silicon layers by outgasing of impurities from the substrate occurred during the cell process.

Illuminated and dark characteristics

After RPHP, three distinct groups of dark IV-curves can be distinguished:

(i) The dark IV-curves of the reference cells, which exhibit quite ideal characteristics.

(ii) The curve of the best solar cell on Si_3N_4 substrate. Its dark saturation currents I_{01} and I_{02} are significantly higher than those of the references, but the parallel resistance R_P with a value of 10^4 Ωcm^2 does not influence the illuminated characteristics dramatically.

(iii) The dark IV-curves of all other cells. Compared to the references, I_{02} is 2-3 orders of magnitude higher, and R_P in the range of 10^2 Ωcm^2 is low enough to have significant detrimental effect. The only sample of type C, has extraordinarily high values of I_{01} and I_{02} which influence V_{oc} dramatically, as well as a very low R_P which negatively influences the fill factor.

After antireflection coating, only the dark characteristics of the latter cell exhibited a significant change: I_{01} and I_{02} were decreased by a factor of 10, and R_P had increased to a value comparable to those of the best cell. The reason for this dramatic improve is unclear.

Only samples of type A and C showed solar cell activity. The best solar cell parameters could be measured for a textured sample of type A with a short circuit current of 26.1 mA/cm^2, an open circuit voltage of 539 mV and a fill factor of 67%, leading to an efficiency of 9.4% with antireflection coating. The best solar cell with a flat surface achieved an efficiency of 8.0 % with an open circuit voltage V_{oc} = 554 mV and a short circuit current I_{sc} = 19.7 mA/cm². Other samples of type A suffered of a low fill factor or a low open circuit voltage, caused by a high I_{02} and low parallel resistance. The following argument which is related to the cracks observed in the silicon layer shall explain this dark parameters:

If one assumes that phosphorous diffusion has taken place inside the cracks up to the bottom of the silicon layer, pn-junctions would have formed in the highly doped BSF region, with diminished extension of the depleted region inside the BSF silicon. Defects then can disturb the depletion region very easily, thus decreasing R_P and increasing I_{02}. This theory is supported strongly by the observation of enhanced current collection along the crack lines detected by SR-LBIC maps (see later), which can only occur if the mean distance to the pn-junction gets shorter for a generated carrier.

None of the samples of type B did show any significant solar cell activity. Impurity contamination can be excluded as a possible reason, since the GDMS measurements proved that their concentrations were comparable to samples of type A. A probable cause for the complete failure of the samples is the combination of severe shunting due to the metal-filled cracks and a high I_{02} due to a bad crystal quality.

Despite the high defect density in the silicon layer, and despite the rather high titanium concentration of the sample of type C, its illuminated characteristics is remarkable, with a measured efficiency of 6.4%. It can be assumed that the lack of cracks in the silicon layer did prevent further deterioration of the cell.

In conclusion, the dark characteristics correlated well with the illuminated characteristics. High I_{02} and low R_P were the most limiting factors for the solar cell performance.

Spectral response

For untextured cells, the light collection properties were similar, as the measurement of the external quantum efficiency proved. It decreases continuously with increasing wavelength, starting at 500 nm.

A low effective minority carrier diffusion length is responsible for this effect, in conjunction with the lack of optical confinement. In contrast to this behavior, the optical confinement due to the random pyramid structure could be clearly observed at the textured cells. In accordance with the spectral light absorption of a 25µm thick silicon layer, the quantum efficiency is enhanced for wavelengths higher than approx. 850 nm.

Spectrally resolved light beam induced current

The electrical characterization of the untextured solar cells on Si_3N_4 ceramic substrates was completed by mapping of the short circuit current density and reflection by the SR-LBIC method and thereby calculation of the minority carrier diffusion length. Mean effective diffusion length was around 16 µm for the best cells (see Fig. 5), and approx. 10 µm for the others.

In the mappings, the cracks of the silicon layer can be found as lines with locally increased effective diffusion length. It is probable, that a locally enhanced current

collection is caused by vertical phosphorous diffusion channels.

The map of the cell on conductive substrate proves that the diffusion length distribution is comparable to that of the best solar cell without surface texture, although no intermediate layer was used for this sample type.

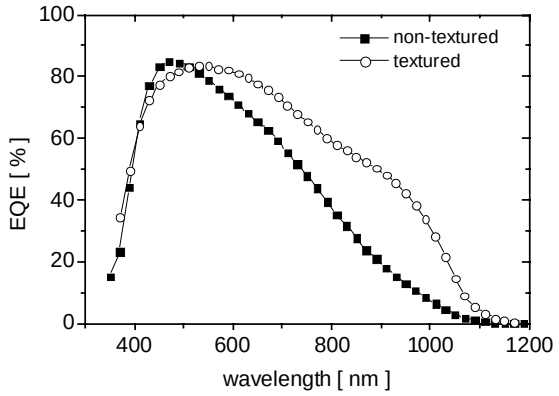

Fig. 4: External quantum efficiency of a solar cell on Si_3N_4 substrate (sample type A) with textured and flat substrate, respectively.

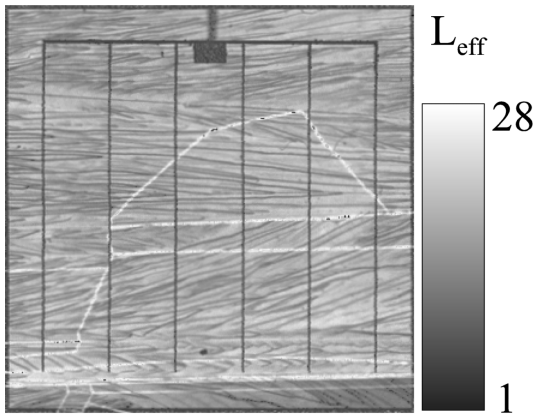

Fig. 5: Diffusion length map of a cell on a type A sample. The bright lines indicate cracks in the silicon layer.

4 SUMMARY

For the first time, CSiTF solar cells on silicon nitride ceramic substrates have been prepared. Si_3N_4 proved to be an excellent and stable substrate for the high-temperature approach with regard to mechanical, chemical and thermal properties. Deposition of all necessary layers could be performed successfully, independent from layer type and deposition temperature. Coarse-grained silicon layers could be achieved by zone-melting recrystallization on samples with intermediate layer. On some samples a tendency to form cracks was observed in the silicon layer during the cool-down cycle of the silicon epitaxy. However, optical, compositional and electrical characterizations proved the high material quality of the silicon layer achieved in this first experiment. On samples with textured surface, solar cell efficiencies up to 9.4% could be achieved, mainly due to the enhanced optical confinement. Thus, silicon nitride ceramics seems to be a very suitable substrate material for future CSiTF solar cell manufacturing.

ACKNOWLEDGMENTS

The authors would like to thank Dr. Wötting of CFI for the preparation of the ceramics samples. Thanks to S. Bau, M. Kwiatkowska, N. Schillinger, H. Lautenschlager, C. Schetter, C. Vorgrimler and G. Emanuel of the Fraunhofer ISE for sample preparation, F.-J. Kamerewerd for GDMS analysis and E. Schäffer for electrical characterization of the cells.

The financial support of the Bayer AG is gratefully acknowledged. The authors are responsible for the content of this publication.

REFERENCES

[1] C. Hebling, et. al., In Proc. 14th European Photovoltaic Solar Energy Conference, ed. by. J. Schmid, H. A. Ossenbrink, P. Helm, H. Ehmann, and E. D. Dunlop (H.S. Stephens, Bedford, UK 1997) p. 2318

[2] A. Takami, et. al., In Proc. 12th European Photovoltaic Solar Energy Conference, ed. by. R. Hill, W. Palz, and P. Helm (H. S. Stephens & Associates, Bedford, UK 1994) p. 59-62

[3] C. Hebling, et. al., Advances in Solid State Physics **38** (1999) 633

[4] R. Monna, et. al., In Proc. 14th European Photovoltaic Solar Energy Conference, ed. by. P. H. H. A. Ossenbrink, H. Ehmann (H.S. Stephens, Bedford, UK 1997) p. 1456

[5] S. Reber, et. al., In Proc. 2nd World Conference on Photovoltaic Solar Energy Conversion, ed. by. J. Schmid, H. A. Ossenbrink, P. Helm, H. Ehmann, and E. D. Dunlop (Joint Research Centre, European Commission, Ispra, Italy 1998) p. 1782

[6] A. v. Keitz, et. al., In Proc. 2nd World Conference on Photovoltaic Solar Energy Conversion, ed. by. J. Schmid, H. A. Ossenbrink, P. Helm, H. Ehmann, and E. D. Dunlop (Joint Research Centre, European Commission, Ispra, Italy 1998) p. 1829

[7] B. v. Ehrenwall, et. al., In Proc. 2nd World Conference on Photovoltaic Solar Energy Conversion, ed. by. J. Schmid, H. A. Ossenbrink, P. Helm, H. Ehmann, and E. D. Dunlop (European Commission, Ispra, Italy 1998) p. 1370

[8] S. Bourdais, et. al., In Proc. 16th European Photovoltaic Solar Energy Conference (2000)

[9] T. Vermeulen, et. al., In Proc. 2nd World Conference on Photovoltaic Solar Energy Conversion, ed. by. J. Schmid, H. A. Ossenbrink, P. Helm, H. Ehmann, and E. D. Dunlop (Joint Research Centre, European Commission, Ispra, Italy 1998) p. 1209

[10] H. Lange, et. al., Angewandte Chemie **103** (1991) 1606-1625

[11] F. L. Riley, Journal of the American Ceramic Society **83** (2000) 245-265

[12] S. Reber, et. al., In Tech. Dig. 11th International Photovoltaic Science and Engineering Conference (Sapporo, Japan, 1999)